IJAME
Int. J. of Applied Mechanics and Engineering, 2023, vol.28, No.1, pp.47-57
DOI: 10.59441/ijame-2023-0005

EVALUATION OF YLT METHOD TO ESTIMATE THE LOAD CARRYING CAPACITY OF ONE-WAY PATCHED REINFORCED CONCRETE SLAB UNDER CONCENTRATED LOAD

Stefanus Adi KRISTIAWAN*, Achmad BASUKI, Agus SUPRIYADI,
Bambang SANTOSA and Sofa MARWOTO
SMARTCrete Research Group, Civil Engineering Department, Universitas Sebelas Maret, Jl. Ir. Sutami No. 36 Surakarta 57126, INDONESIA
E-mail: s.a.kristiawan@ft.uns.ac.id

An unsaturated polyester resin (*UPR*) mortar was applied to repair the damage to the tension zone's one-way reinforced concrete (*RC*) slabs. The load carrying capacity of the patched RC slab is of interest to justify the effectiveness of the repair. The Yield Line Theory (*YLT*) may be used to estimate the load carrying capacity of patched RC slabs under concentrated load. The results of the *YLT* are compared with the experimental results to evaluate the validity of the *YLT* method. The results confirm that patching alters the yield line formation, mainly when the concentrated load is applied close to the patching zone. Subsequently, the *YLT* method provides a higher load carrying capacity estimation deviation for slabs with a loading point near the patching zone. On the other hand, the *YLT* method estimates load carrying capacity accurately when the loading point is away from the patching zone.

Key words: load carrying capacity, one-way slab, patch repair, reinforced concrete, *YLT* .

1. Introduction

An *RC* slab must be designed in such a way to meet the strength and serviceability requirements as set by the Codes. However, the slab may not fulfill the requirements after years of service. Degradation of the concrete could be the reason, for example, the occurrence of cracking and delamination of concrete cover due to reinforcement corrosion [1, 2]. Another type of damage is spalling of the concrete cover as a result of fire [3]. In such circumstances, the repair is necessary to restore the performance and durability of the slab. The choice of repair depends on the degradation type and the intended restoration level. A patching method can be selected to restore the spalling and delamination of the *RC* slab. The repair requires a compatible material with the existing concrete [4].

The primary purpose of patching is to replace the concrete spalling or delamination with a repair material to recover the damaged element's size [5]. Restoring the size of the damaged element is sufficient to protect the element from further deterioration. However, to restore strength and serviceability, the repair material should have mechanical compatibility with the parent concrete [6, 7]. Thus, it is essential to develop a repair material that can be applied to recover the size and regain the strength and serviceability of the damaged element to its original condition [8]. Otherwise, other repairs or strengthening systems must be implemented [9-13]. Previous research successfully developed a repair material using UPR-mortar [14], which can restore the load carrying capacity of the damaged *RC* slabs [15, 16]. This material is used in this research to repair damaged slabs, and their subsequent load carrying capacity is of interest.

Theoretically, the ultimate capacity of the *RC* slab can be estimated by various methods. One of such methods is the Yield Line Theory (*YLT*) [17-22]. This theory can be explained as follows (see Fig.1). Under

* To whom correspondence should be addressed

concentrated load, a crack is induced in the slab to form a line of rotation, causing failure of the slab. The yield line divides the slab into two segments. Based on the principle of energy equilibrium (internal work W_i equals external work W_e), the ultimate load P_u may be calculated by the virtual work method as given in Eq.(1.1):

$$\sum m_{un}.\theta_n.L_o = \sum P_u.\Delta \tag{1.1}$$

where the left-hand and right-hand sides of the equation represent respectively the internal and external work, m_{un} is the ultimate bending moment capacity of the slab, θ_n is the rotation angle of the two slab segments, and L_0 is the length of the yield line. The rotation angle θ_n can be determined from Eq.(1.2) as follows (see Fig.1):

$$\theta_n = \frac{\Delta}{b_1} + \frac{\Delta}{b_2} \tag{1.2}$$

where Δ is the deflection along the yield line.

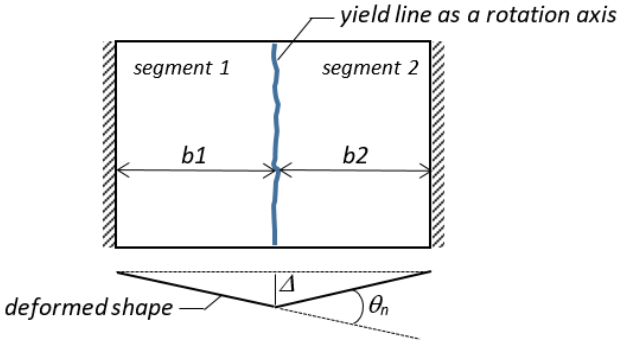

Fig.1. Rotation of slab segments (θ_n) about each yield line.

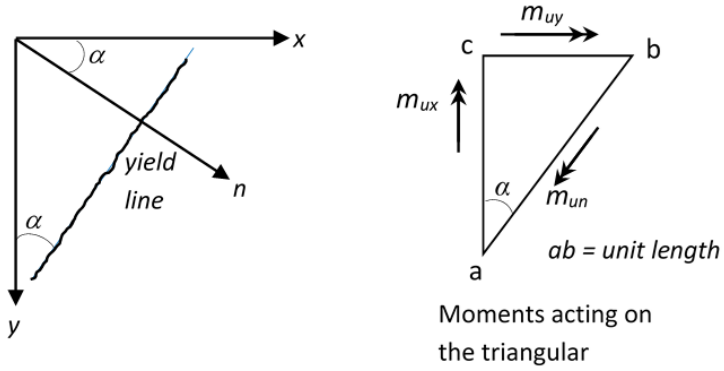

Fig.2. Yield line at a general angle to orthogonal slab reinforcement.

In some instances, the ultimate bending moment capacity (m_{un}) along the yield line may not be in the same direction as the reinforcement axis (see Fig.2). For this case, the ultimate bending moment capacity can be determined by Eq.(1.3)

$$m_{un} = m_{ux}cos^2\alpha + m_{uy}sin^2\alpha\,. \tag{1.3}$$

The accuracy of the *YLT* method in estimating the load carrying capacity of the *RC* slab is influenced by the correct estimation of the yield lines pattern. Previous studies indicated that repair material alters the formation of the yield lines in the patched *RC* slab [15, 23]. For this reason, this research aims to evaluate the validity of the *YLT* for estimating the load carrying capacity of one-way patched *RC* slabs under a concentrated load.

2. Materials and method

This research used four slabs of *1350x800x80mm* size. The slabs were cast in such a way as to create a cut-out to simulate damage in the tensile zone.

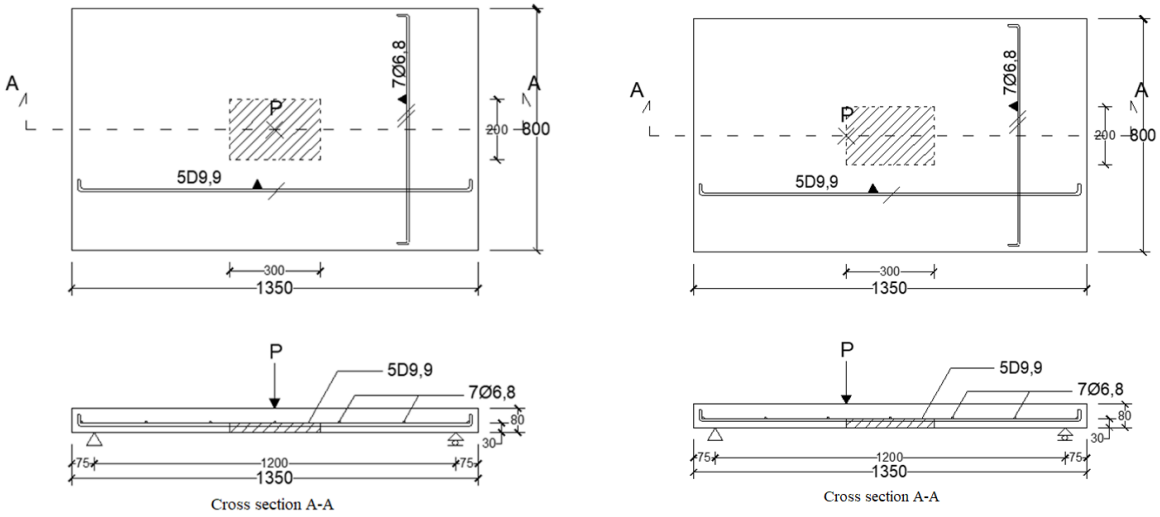

a. R1 *RC* slab b. R2 *RC* slab

c. R3 *RC* slab d. R4 *RC* slab

Fig.3. Reinforcements layout of patched *RC* slabs and their loading point *P*.

The cut-out was *300x200x30mm* and located right in the center of the slabs. After *90* days, the *UPR* -mortar was applied to fill the cut-out. The *UPR* -mortar was of the following composition: *860.7kg* of sand, *430.4kg* of *UPR* , *731.6kg* of cement, and *129.1kg* of fly ash. Five reinforcements with a diameter of 9.9*mm* (5D9.9) were provided to reinforced slabs in the longitudinal axis. Meanwhile, 7D6.8 reinforced slabs in the vertical axis. Figure 3 illustrates the slab and its reinforcements layout. The properties of concrete, *UPR* -mortar, and reinforcement are given in Table 1.

Each slab was tested by applying a load *P* at an increment of *0.5kN* until failure. For each slab, the load was applied at a different loading point (see Fig.3). The corresponding deflection of the slab under the loading point was monitored using dial gauges. The longitudinal reinforcement strain at the center of the slab was measured using a strain gauge. The formation of yield lines pattern at failure was noted.

Table 1. Materials properties.

Material	**Compressive Strength** (*MPa*)	**Tensile Strength** (*MPa*)	**Elastic modulus** (*GPa*)
Concrete	*23.74*	*3.45*	*22.85*
UPR -mortar	*71.16*	*20.80*	*15.75*
Reinforcement	-	*350.50*	*200.00*

3. Results and discussion

3.1. General behavior

The behavior of patched *RC* slabs under a concentrated load is expressed in terms of load-deflection curves, as shown in Fig.4. The curves follow the general pattern of a flexural element behavior, i.e., initially, the element demonstrates high stiffness where an increase in load causes a proportionally slight increase in deflection. After reaching a specific limit, the element's stiffness decreases, indicated by a change in the slope of the curve. This behavior can be related to the formation of the initial crack in the slabs. Subsequently, a further load increase induces higher stress in the reinforcements and triggers plastic behavior at the final stage except for the R1 slab. For this particular specimen, separation of the patch repair material and the concrete substrate has occurred (see Section 3.2). Subsequently, the R1 specimen could not take a higher load after the delamination.

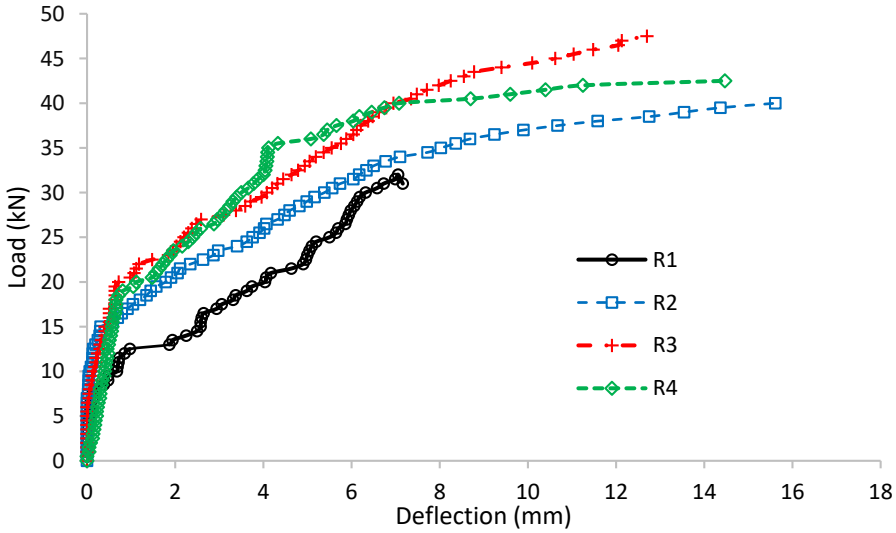

Fig.4. Load-deflection behavior of patched *RC* slabs.

Figure 5 shows the longitudinal reinforcement strain at the center of the patched *RC* slabs. The observed reinforcement strain of R1 and R2 specimens indicates that the reinforcements attain a yielding state, while the reinforcement strain in the other slabs (R3 and R4) does not show such a state. The explanation is as follows: for R3 and R4, the strain gauge was installed away from the center of cracks formation (see Section 3.2). So no localized stress was observed in this particular spot of reinforcements. Subsequently, the yielding state cannot be identified in these reinforcements. However, if the strain gauge was installed near the center of cracks formation, it would be expected to confirm the occurrence of plastic state in the R3 and R4 specimens.

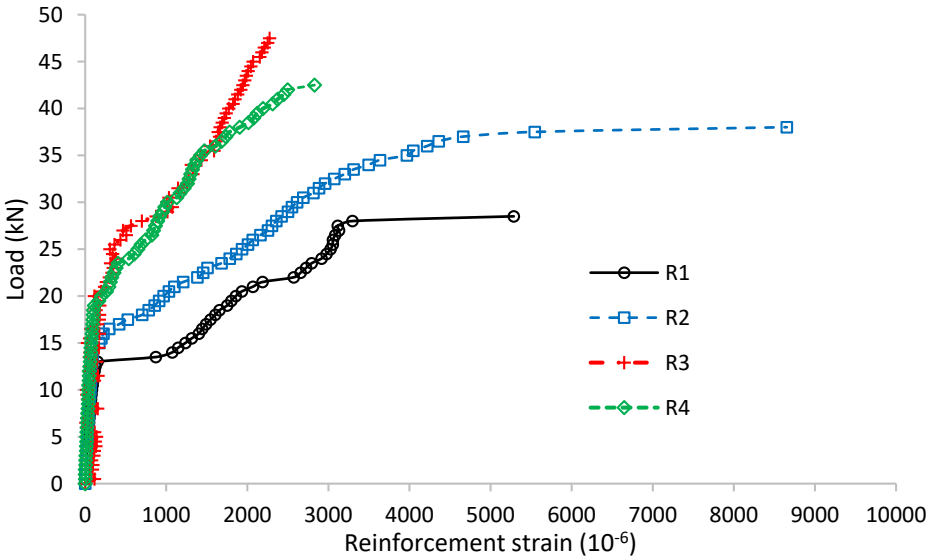

Fig.5. Load-reinforcement strain of patched RC slabs.

Referring to Figs 4 and 5, the main findings are as follows: all slabs fail at ultimate load by a flexural failure mode where the failure is preceded by reinforcing steel reaching a yield state except for the R1 specimen. For the R1 slab, the delamination causes the yielding of reinforcing steel at a lower load than expected. The failure mode and its corresponding ultimate load of the slabs will be used as a control in the subsequent analysis.

3.2. Yield lines pattern

Figure 6 shows the cracks formation of patched *RC* slabs investigated in this study. Cracks occur in the tensile zone and initially arise just below the loading point. From this point, cracks tend to propagate radially toward the slabs' edge except for the R1 specimen. It is also interesting to note that cracks do not arise in the repair material since it is made of the *UPR* -mortar with outstanding tensile strength $(20.8MPa)$. The repair material alters the crack propagation, i.e., the crack path is disrupted as it passes through the repair material. The closer the repair material is to the center of the crack formation, the greater the effect of the repair material in interfering with the crack formation. The alteration causes, for example, that the crack formation of the R1 slab tends to be linear and parallel.

In addition to non-radial cracks formation, the cracks of the R1 slab are also less intense than the other slabs. Careful inspection of the failure mode of the R1 specimen indicates that delamination of the repair material occurred, as shown in Fig.7. The delamination may be triggered by the fact that the patching material in the R1 specimen did not fully seal the repair zone, leaving a gap between repair material and concrete (see Fig.7.a). Therefore, the R1 specimen fails to maintain the integrity of the repair zone. Subsequently, the imposed load after delamination does not induce a new formation of crack; instead, the existing cracks are

widening and the delamination is more significant. On the contrary, other specimens do not show any delamination. Thus, the stress due to the imposed load could be well redistributed to intensify crack formation.

The crack paths at failure can be viewed as the yield lines where the maximum moment in the slab induces the yielding of the reinforcements at crossing the crack paths. The observed reinforcement strains close to the crack paths of the R1 and R2 specimens confirm this, as discussed in the preceding section. Thus, the cracking pattern of slabs at failure will be used to identify the yield lines in the subsequent analysis.

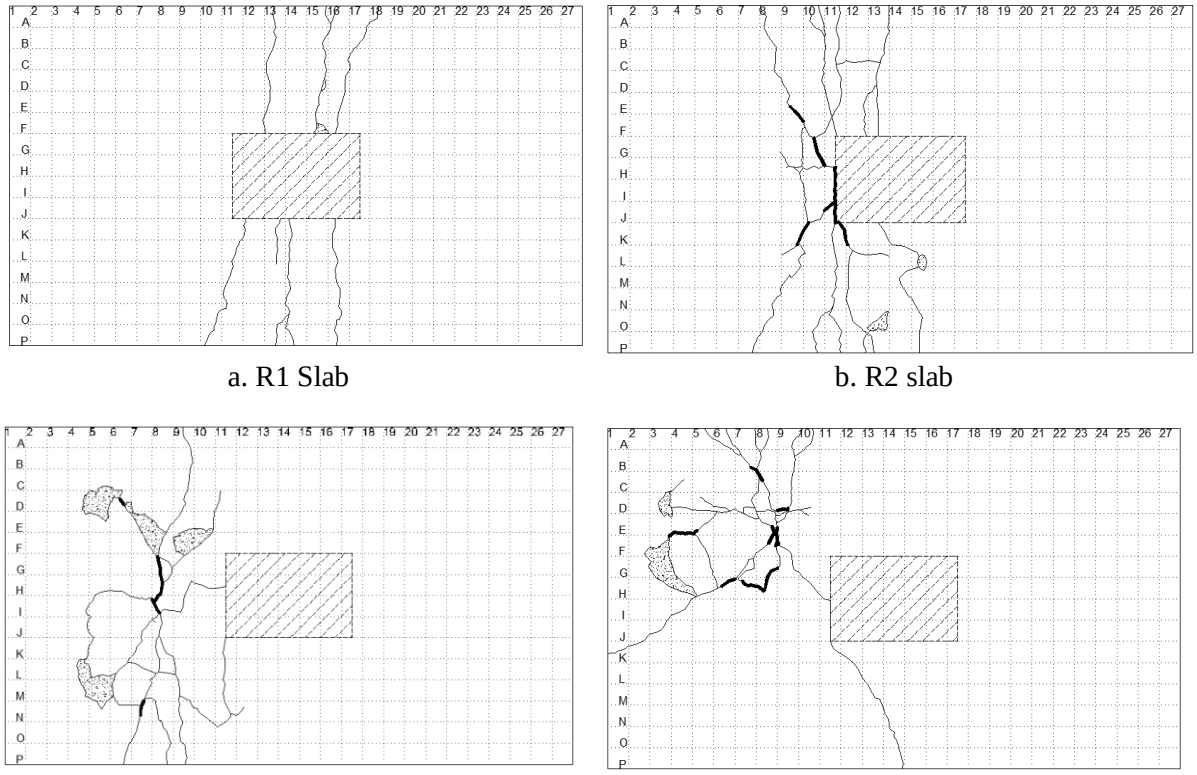

a. R1 Slab b. R2 slab

c. R3 slab d. R4 slab

Fig.6. Cracks formation of patched RC slabs at failure.

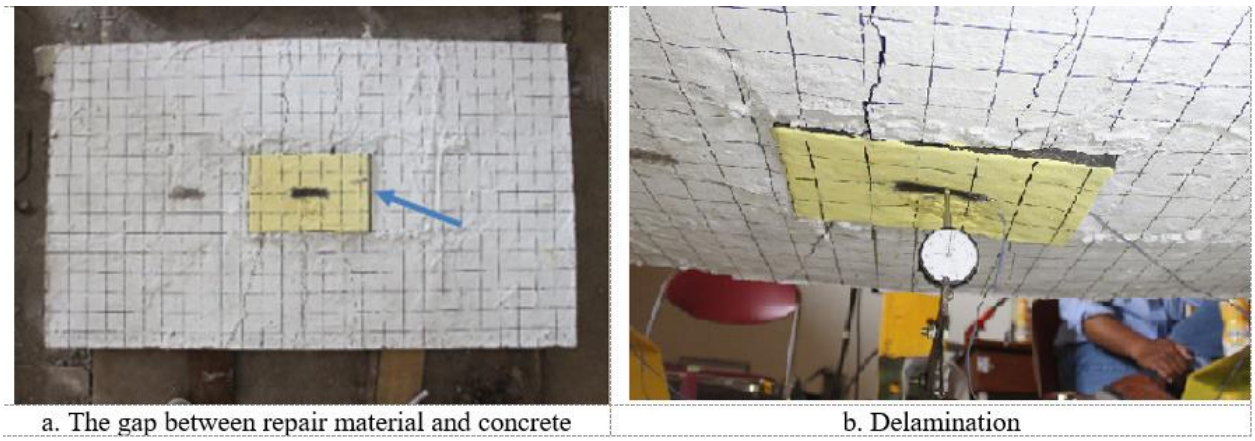

a. The gap between repair material and concrete b. Delamination

Fig.7. Delamination of repair material in R1 specimen.

3.3. Estimated load carrying capacity by the *YLT* method

The first step in estimating the load carrying capacity of the slab based on the *YLT* method (i.e., using Eq.(1.1)) is to determine the yield lines (*YL*) and their respective orientation (α) to the reinforcement axis. In this case, axes parallel to the longitudinal and vertical reinforcements are defined as *X* and *Y* axes, respectively (see Fig.8). Another parameter that should be determined from the yield line patterns is the length component b_i, which is then used to calculate the rotation angle θ_n of the corresponding yield line using Eq.(1.2). The calculation requires the deflection Δ under the loading point, and its value can be obtained from Fig.4.

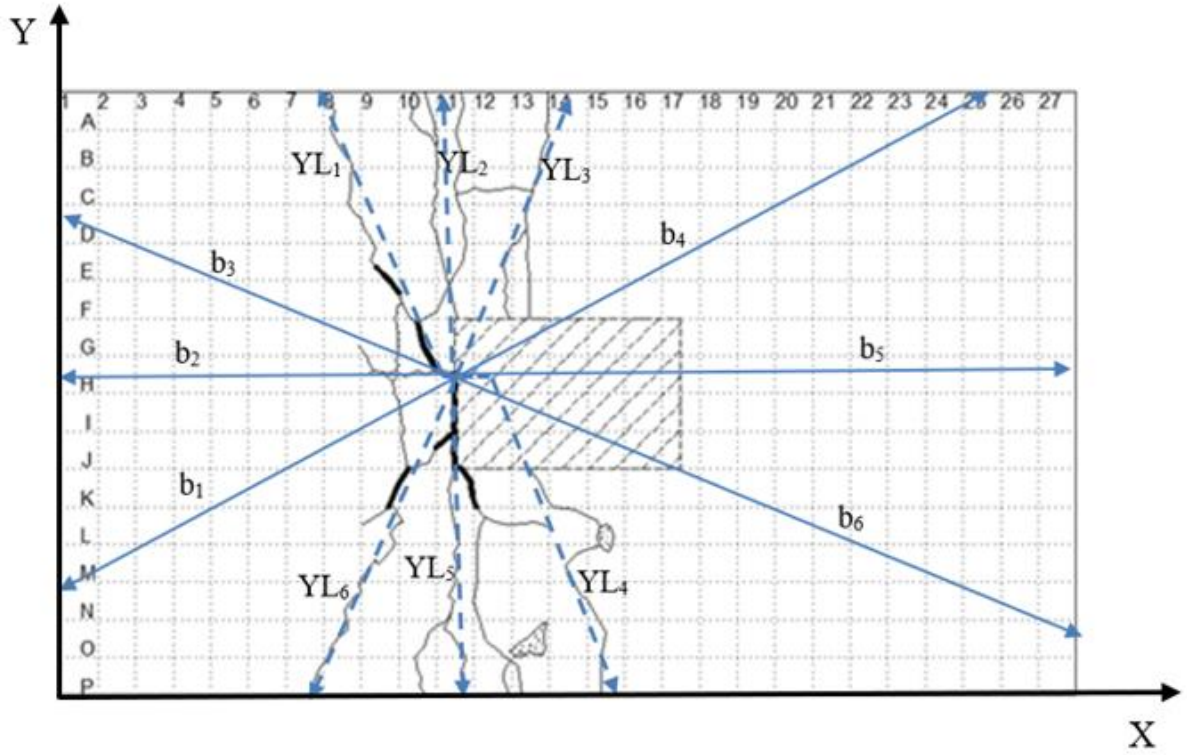

Notation:
YL_i = the i^{th} yield line
b_1-b_4 = length component to calculate the rotation angle θn of YL_1 and YL_4
b_2-b_5 = length component to calculate the rotation angle θn of YL_2 and YL_5
b_3-b_6 = length component to calculate the rotation angle θn of YL_3 and YL_6

Fig.8. The yield line patterns and their corresponding parameters.

Calculating slab load carrying capacity using Eq.(1.1) also requires the ultimate bending moment capacity (m_{un}) as the input parameter. For slabs without compression reinforcements layout, the ultimate bending moment capacity can be determined using Eqs (3.1) and (3.2):

$$m_{un} = A_s f_y \left(d - a/2\right), \tag{3.1}$$

$$a = \frac{A_s f_y}{0.85 f_c^{'} b} \tag{3.2}$$

where A_s is the reinforcement area, f_y is the reinforcement yield strength, d is the slab effective depth, a is the depth of the equivalent compression zone, $f_c^{'}$ is the concrete compressive strength, and b is the slab width. Referring to Fig.8, the yield lines do not orientate the same as the reinforcement axis. Therefore, m_{un} has to be calculated by Eq.(1.3). The ultimate bending moment in the direction of the X (m_{ux}) and Y (m_{uy}) axes must be determined first, as follows: the reinforcements along the X direction are 5D9.9, and so the total reinforcement area is $384.69mm^2$. The yield strength of the reinforcement is $350.5MPa$, while the concrete compressive strength is $29.4MPa$. With an effective depth of $47mm$, the ultimate bending moment per unit length in this direction (m_{ux}) is $7,353,118N.mm$. In the same way, with the reinforcements along the Y direction being 7D6.8 and the effective depth of *52mm*, the ultimate bending moment per unit length in this direction (m_{uy}) is $5,652,109\,N.mm$. Table 2 shows the summary of load carrying capacity calculation of the slabs by the YLT method. In this table, only four yield lines of the R4 slab can be identified based on its cracking pattern shown in Fig.6.d.

Table 2. Summary of load carrying capacity calculation of the slabs by the YLT method.

Slab	*YL*	α (°)	m_{un} (N.mm)	L_0 (m)	Δ (mm)	*b1* (mm)	*b2* (mm)	θ_v (ραδ)	W_i (N.mm)	$\sum Wi$ *(N.mm)*	P_u (kN)	$P_{u,ex}$ (kN)	*R*
R1	*YL-1*	*20*	*5935379*	*0.308*	*7.16*	*607*	*809*	*0.0207*	*37740*	*252619*	*35.27*	*31*	*1.14*
	YL-2	*0*	*7353118*	*0.299*		*686*	*668*	*0.0212*	*46522*				
	YL-3	*0*	*7353118*	*0.299*		*747*	*615*	*0.0212*	*46651*				
	YL-4	*3*	*7319242*	*0.299*		*809*	*607*	*0.0207*	*45209*				
	YL-5	*5*	*5788979*	*0.299*		*668*	*686*	*0.0212*	*36626*				
	YL-6	*20*	*5935379*	*0.316*		*615*	*747*	*0.0212*	*39871*				
R2	*YL-1*	*25*	*7323321*	*0.429*	*15.61*	*524*	*714*	*0.0517*	*162148*	*805655*	*51.60*	*40*	*1.29*
	YL-2	*5*	*5788979*	*0.333*		*476*	*724*	*0.0544*	*104889*				
	YL-3	*6*	*7220315*	*0.333*		*505*	*790*	*0.0507*	*121978*				
	YL-4	*30*	*5692582*	*0.429*		*714*	*524*	*0.0517*	*126042*				
	YL-5	*0*	*7353118*	*0.476*		*724*	*476*	*0.0544*	*190327*				
	YL-6	*20*	*5935379*	*0.333*		*790*	*505*	*0.0507*	*100271*				
R3	*YL-1*	*10*	*6849689*	*0.404*	*12.70*	*369*	*1011*	*0.0470*	*130072*	*609464*	*47.99*	*47.5*	*1.01*
	YL-2	*12*	*6863379*	*0.396*		*360*	*1020*	*0.0477*	*129483*				
	YL-3	*27*	*5797281*	*0.264*		*440*	*791*	*0.0449*	*68717*				
	YL-4	*8*	*5688120*	*0.413*		*1011*	*369*	*0.0470*	*110363*				
	YL-5	*25*	*7323321*	*0.264*		*1020*	*360*	*0.0477*	*92107*				
	YL-6	*30*	*5692582*	*0.308*		*791*	*440*	*0.0449*	*78722*				
R4	*YL-1*	*52*	*5697298*	*0.505*	*14.47*	*446*	*539*	*0.0593*	*170616*	*645100*	*44.58*	*42.5*	*1.05*
	YL-2	*30*	*5692582*	*0.337*		*312*	*707*	*0.0669*	*128275*				
	YL-3	*20*	*5935379*	*0.261*		*421*	*1011*	*0.0487*	*75436*				
	YL-4	*NA*	*0*	*0.000*		*0*	*0*	*0*	*0*				
	YL-5	*40*	*6408728*	*0.632*		*707*	*312*	*0.0669*	*270773*				
	YL-6	*NA*	*0*	*0.000*		*0*	*0*	*0*	*0*				

Comparisons between the analytical (P_u) and experimental ($P_{u,ex}$) load carrying capacity results are expressed in ratio R. This research shows that the analytical method gives a higher load carrying capacity than the experimental result for all cases, with the ratio within the $1-5$ % range for the R3 and R4 slabs and the $14-29$% range for the R1 and R2 slabs. A careful inspection of the cracking pattern shown in Fig.6 confirms that the position of the loading point to the patching zone influences the cracking formation. Thus, the patch repair affects the length and orientation of the yield lines of the R1 and R2 slabs, but it hardly influences the yield lines of the R3 and R4 slabs. Consequently, the impact of patch repair on the calculation of load carrying capacity by *YLT* method is more pronounced for the R1 and R2 slabs than for the R3 and R4 slabs.

4. Conclusions

The following conclusions are made:

- The behavior of the patched *RC* slab is similar to the general behavior of a flexural element.
- Cracks are started right under the concentrated load and propagate radially from this point.
- The presence of the repair material alters the propagation of the cracks, especially when the repair material is close to the loading point.
- The observed reinforcement strain near the loading point indicates that it attains a plastic state. This suggests that the primary crack propagation forms the yield lines.
- The *YLT* method estimates the load carrying capacity accurately when the loading point is away from the patching zone. On the contrary, it gives a higher diverted estimation when the loading point is applied near the patching zone due to the alteration of yield line formation.

Acknowledgement

This research has been made possible due to financial support by Universitas Sebelas Maret through Hibah Grup Riset (contract No.254/UN27.22/PT.01.03/2022).

Nomenclature

a – equivalent compression zone depth
A_s – reinforcement area
α – angle between yield line and primary axis
b – slab width
b_i – length component to calculate rotation angle
d – effective slab depth
Δ – slab deflection
$f_c^{'}$ – concrete compressive strength
f_y – reinforcement yield strength
L_0 – yield line length
m_{un} – ultimate bending capacity
m_{ux} – ultimate bending capacity in the longitudinal direction (X-axis)
m_{uy} – ultimate bending capacity in the vertical direction (Y-axis)
P – concentrated load
P_u – analytical load carrying capacity

$P_{u,ex}$ – experimental load carrying capacity

θ_n – rotation angle

R – analytical and experimental load carrying capacity ratio

RC – reinforced concrete

UPR – unsaturated polyester resin

W_e – external energy

W_i – internal energy

YL – yield line

YLT – yield line theory

References

[1] Mullard J. A. and Stewart M. G. (2011): *Corrosion-induced cover cracking: New test data and predictive models.*– ACI Struct. J., vol.108, No.1, pp.71-79. doi: 10.14359/51664204.

[2] LiC. Q., Zheng J. J., Lawanwisut W. and Melchers R. E. (2007): *Concrete delamination caused by steel reinforcement corrosion*.– J. Mater. Civ. Eng., vol.19, No.7, pp.591-600. doi: 10.1061/(ASCE)0899-1561(2007)19:7(591).

[3] McNamee R., Sjöström J. and Boström L. (2021): *Reduction of fire spalling of concrete with small doses of polypropylene fibres*.– Fire Mater., vol.45, No.7, pp.943-951. doi: 10.1002/fam.3005.

[4] Logeswaran V. and Ramakrishna G. (2020): *A study on compatibility of concrete repair materials.*– J. Xi'an Univ. Archit. Technol., vol.12, No.6, pp.1123-1143.

[5] KimH., Han D., Kim K. and Romero P. (2020): *Performance assessment of repair material for deteriorated concrete slabs using chemically bonded cement*.– Constr. Build. Mater., vol.237, p.117468. doi: 10.1016/j.conbuildmat.2019.117468.

[6] Nunes V. A., Borges P.H.R. and Zanotti C. (2019): *Mechanical compatibility and adhesion between alkali-activated repair mortars and Portland cement concrete substrate.*– Constr. Build. Mater., vol.215, pp.569-581. doi: 10.1016/j.conbuildmat.2019.04.189.

[7] Venkiteela G., Klein M., Najm H. and Balaguru P. N. (2017): *Evaluation of the compatibility of repair materials for concrete structures.*– Int. J. Concr. Struct. Mater., vol.11, No.3, pp.435-445. doi: 10.1007/s40069-017-0208-5.

[8] Río O., Andrade C., Izquierdo D. and Alonso C. (2005): *Behavior of patch-repaired concrete structural elements under increasing static loads to flexural failure*.– J. Mater. Civ. Eng., vol.17, No.2, pp.168-177. doi: 10.1061/(asce)0899-1561(2005)17:2(168).

[9] Koutas L. N. and Bournas D. A. (2017): *Flexural strengthening of two-way rc slabs with textile-reinforced mortar: experimental investigation and design equations.*– J. Compos. Constr., vol.21, No.1, p. 04016065. doi: 10.1061/(ASCE)CC.1943-5614.0000713.

[10] Fernandes H., Lúcio V. and Ramos A. (2017): *Strengthening of RC slabs with reinforced concrete overlay on the tensile face.*– Eng. Struct., vol.132, pp.540-550. doi: 10.1016/j.engstruct.2016.10.011.

[11] Al-Rousan R. (2019): *Behavior of two-way slabs subjected to drop-weight.*– Mag. Civ. Eng., vol.90, No.6, pp.62-71. doi: 10.18720/MCE.90.6.

[12] Yin H., Teo W. and Shirai K. (2017): *Experimental investigation on the behaviour of reinforced concrete slabs strengthened with ultra-high performance concrete.*– Constr. Build. Mater., vol.155, pp.463-474. doi: 10.1016/j.conbuildmat.2017.08.077.

[13] Zheng Y., Yu G. and Pan Y. (2012): *Investigation of ultimate strengths of concrete bridge deck slabs reinforced with GFRP bars.*– Constr. Build. Mater., vol.28, No.1, pp.482-492. doi: 10.1016/j.conbuildmat.2011.09.002.

[14] Adi Kristiawan S. and Bekti Prakoso A. (2016): *Flexural behaviour of patch-repair material made from unsaturated polyester resin (UPR)-Mortar.*– Mater. Sci. Forum, vol.857, pp.426-430. doi: 10.4028/www.scientific.net/MSF.857.426.

[15] Kristiawan S., SupriyadiA., Pradana D. R. and Azhim M. R. N. (2018): *Flexural behaviour of one-way patched reinforced concrete (RC) slab under concentrated load*.– Asian J. Civ. Eng., vol.19, No.2. doi: 10.1007/s42107-018-0014-7.

[16] Kristiawan S. A. and Supriyadi A. (2020): *Two-way patched RC slabs under concentrated loads*.– Mag. Civ. Eng., vol.94, No.2, pp.108–119. doi: 10.18720/MCE.94.9.

[17] Quintas V. (2003): *Two main methods for yield line analysis of slabs*.– J. Eng. Mech., vol.129, No.2, pp.223–231. doi: 10.1061/(ASCE)0733-9399(2003)129:2(223).

[18] Deaton J. B. (2005): *A Finite Element Approach to Reinforced Concrete Slab Design*.– MSc Thesis, Georgia Institute of Technology.

[19] Alasam M. A. A. (2006): *Yield Line Method Applied to Slabs with Different Supports.* MSc Thesis, University of Khartoum.

[20] Salehian H. and Barros J. A. O. (2017): *Prediction of the load carrying capacity of elevated steel fibre reinforced concrete slabs*.– Compos. Struct., vol.170, pp.169-191. doi: 10.1016/j.compstruct.2017.03.002.

[21] Bauer D. and Redwood R. G. (1987): *Numerical yield line analysis*.– Comput. Struct., vol.26, No.4, pp.587–596. doi: 10.1016/0045-7949(87)90007-1.

[22] Burgess I. (2017): *Yield-line plasticity and tensile membrane action in lightly-reinforced rectangular concrete slabs*.– Eng. Struct., vol.138, pp.195-214. doi: 10.1016/j.engstruct.2017.01.072.

[23] Taouche-Kheloui F., Djellad Z. A., Tahar K. A. and Bélaidi O. (2015): *Behavior of concrete slabs reinforced with composite patch under centric punching load*.– Procedia Eng., vol.114, pp.255-262. doi: 10.1016/j.proeng.2015.08.066.

Received: August 9, 2022
Revised: January 17, 2023